AGU PUBLICATIONS

Geophysical Research Letters

RESEARCH LETTER
10.1002/2017GL074561

Key Points:
- With CO_2 doubling, the ocean heat flux convergence shifts poleward in winter in both hemispheres
- These changes in the ocean heat flux convergence amplify polar warming and damp extrapolar warming
- Decreased extrapolar warming contributes to the enhanced high-latitude lapse rate feedback

Supporting Information:
- Supporting Information S1

Correspondence to:
H. A. Singh,
hansi.singh@pnnl.gov

Citation:
Singh, H. A., Rasch, P. J., & Rose, B. E. J. (2017). Increased ocean heat convergence into the high latitudes with CO_2 doubling enhances polar-amplified warming. *Geophysical Research Letters*, *44*. https://doi.org/10.1002/2017GL074561

Received 13 JUN 2017
Accepted 25 AUG 2017
Accepted article online 1 SEP 2017

Increased Ocean Heat Convergence Into the High Latitudes With CO_2 Doubling Enhances Polar-Amplified Warming

H. A. Singh[1], P. J. Rasch[1], and B. E. J. Rose[2]

[1] Atmospheric Science and Global Change Division, Pacific Northwest National Laboratory, U.S. DOE Office of Science, Richland, Washington, USA, [2]Department of Atmospheric and Environmental Sciences, State University of New York at Albany, Albany, New York, USA

Abstract We isolate the role of the ocean in polar climate change by directly evaluating how changes in ocean dynamics with quasi-equilibrium CO_2 doubling impact high-latitude climate. With CO_2 doubling, the ocean heat flux convergence (OHFC) shifts poleward in winter in both hemispheres. Imposing this pattern of perturbed OHFC in a global climate model results in a poleward shift in ocean-to-atmosphere turbulent heat fluxes (both sensible and latent) and sea ice retreat; the high latitudes warm, while the midlatitudes cool, thereby amplifying polar warming. Furthermore, midlatitude cooling is propagated to the polar midtroposphere on isentropic surfaces, augmenting the (positive) lapse rate feedback at high latitudes. These results highlight the key role played by the partitioning of meridional energy transport changes between the atmosphere and ocean in high-latitude climate change.

1. Introduction

The impact of ocean dynamics on polar climate evolution remains uncertain. Many studies suggest a prominent role for the ocean in high-latitude climate sensitivity. Increased ocean heat transport into the Arctic correlates positively with Arctic amplification in climate model intercomparison studies (Holland & Bitz, 2003; Hwang et al., 2011; Mahlstein & Knutti, 2011), while atmospheric moist static energy transport changes are negatively correlated (Hwang et al., 2011). In the Antarctic, anthropogenic forcings (both greenhouse gas increase and stratospheric ozone depletion) have stimulated increased heat uptake over the Southern Ocean (Purkey & Johnson, 2010), acting to damp surface warming both locally and globally (Rose et al., 2014). Indeed, polar climate warming is more symmetric between hemispheres when ocean dynamics are held fixed (Bitz et al., 2006), suggesting that differences in the transient ocean response may elicit the very different Arctic and Antarctic climate sensitivities found when atmosphere and ocean are coupled.

Despite evidence that ocean dynamics are a key factor in polar climate change, radiative feedback studies present a less consistent picture of the ocean's role. Both Winton (2006) and Pithan and Mauritsen (2014) show that longwave temperature feedbacks dominate high-latitude warming and amplification, while the ice-albedo feedback plays a less central role than previously assumed (see, e.g., Manabe & Wetherald, 1975). Indeed, that winter warming greatly exceeds summer warming in the Arctic suggests a greater role for processes that operate in polar night, including longwave feedbacks and dynamic energy transports. While Winton (2006) finds that the change in the total meridional energy transport into the Arctic is nearly as important to Arctic amplification as the temperature longwave feedbacks, Pithan and Mauritsen (2014) find that neither ocean nor atmospheric energy transports contribute substantially to polar amplification compared to the high-latitude lapse rate feedback.

Nummelin et al. (2017) propose that the discrepancy between radiative feedback calculations, such as that performed by Pithan and Mauritsen (2014), and studies like Holland and Bitz (2003) that link Arctic amplification to ocean heat transport changes is due to the spatial heterogeneity of the ocean heat transport (OHT) response to CO_2-induced warming. In the Northern Hemisphere (NH), OHT decreases in the tropics and midlatitudes, remains unchanged in the subpolar regions, and increases in the Arctic itself; therefore, as expected, the covariance between polar amplification and OHT depends on the region in which both are measured

Table 1
Description of Slab Ocean Model (SOM) Experiments

Experiment name	Atmospheric state	Ocean state
Control	$1XCO_2$	Control OHFC
PertAtm	$2XCO_2$	Control OHFC
PertOcn	$1XCO_2$	Perturbed ($2XCO_2$) OHFC
PertAtm+PertOcn	$2XCO_2$	Perturbed ($2XCO_2$) OHFC

Note. "Perturbed ($2XCO_2$) OHFC" indicates that the ocean fluxes prescribed in the slab ocean model are derived from the 2XCO2_300yr (CO_2 doubling following 300) experiment rather than a preindustrial control as in the "Control OHFC" case.

(Holland & Bitz, 2003; Nummelin et al., 2017). These findings suggest that the ocean's role in polar warming is best assessed holistically: how do changes in global ocean dynamics linked to CO_2-induced warming impact the climate system, and more specifically, the high latitudes?

In this study, we consider the role of changing ocean dynamics in the polar climate response to CO_2 doubling in both hemispheres. We focus on winter and show that at quasi-equilibrium, CO_2-induced warming produces similar changes in the ocean heat flux convergence (OHFC) in the Arctic and Antarctic. We analyze the climatic impact of this OHFC change by imposing it in a slab ocean model framework and use local feedback analysis techniques to isolate mechanisms (both local and remote) by which changing ocean dynamics impacts polar climates.

2. Experimental Design

The quasi-equilibrium ocean response to CO_2 doubling is computed by running a fully coupled configuration of the Community Earth System Model version 1.1 (CESM1) (Hurrell et al., 2013) at nominally 1° spatial resolution with components as follows: Community Atmosphere Model version 5 (CAM5) (Neale et al., 2012); the Parallel Ocean Program version 2 (Danabasoglu et al., 2012), which utilizes the subgrid-scale eddy parameterization of Gent and McWilliams (1992); the Los Alamos Sea Ice Model (Hunke & Lipscomb, 2008); and the Community Land Model version 4 (Oleson et al., 2010). Branching from a preindustrial control run (piC), carbon dioxide is doubled abruptly from its preindustrial levels (284 to 568 ppm) for 330 years, with all other parameters held constant ($2XCO_2$_300 yr). The climatology is computed over the final 30 years of the simulation. The net top-of-atmosphere energy imbalance from years 300 to 330 is 0.2 W m^{-2}, indicating that net ocean heat uptake is small and the simulation is close to radiative equilibrium.

The ocean heat flux convergence (OHFC) monthly fields are computed from the fully coupled piC run (Cont OHFC) and the 2XCO2_300yr run (Pert OHFC) using the "Q-flux" formulation described by Bitz et al. (2012)

$$\rho_w c_p h_{\mathrm{ML}} \frac{\mathrm{d}T_{\mathrm{ML}}}{\mathrm{d}t} = F_{\mathrm{net}} - Q_{\mathrm{flx}}, \tag{1}$$

where Q_{flx} is the OHFC, F_{net} is the net surface heat flux, T_{ML} is the temperature of the mixed layer, c_p is the heat capacity of seawater, and ρ_w is the density of seawater. The mixed layer depth, h_{ML}, is taken to be the annual mean depth following Bailey et al. (2010).

Four CESM1 experiments utilizing a slab ocean model (SOM) are performed, as outlined in Table 1, with either Cont OHFC or Pert OHFC prescribed in the SOM and with CO_2 held at either its preindustrial concentration (1XCO2) or doubled (2XCO2). The slab ocean framework permits the role of ocean dynamics in the climate system response to be isolated by substituting the SOM (with a prescribed monthly varying Q_{flx}) in place of the fully dynamic ocean model. The SOM is incapable of moving heat, either vertically or laterally, other than as parameterized through the prescribed OHFC. Since the ocean dynamics are prescribed and cannot change, the elements of the climate system response attributable to a particular ocean state can be identified.

In PertAtm (2XCO2, Cont OHFC; see Table 1), the ocean is not allowed to respond to atmospheric CO_2 doubling, thereby isolating parts of the climate system response that are independent of changes in ocean dynamics. On the other hand, PertOcn (1XCO2, Pert OHFC) isolates the climate impact of the ocean response to CO_2 doubling, apart from other changes rendered by CO_2 doubling. Finally, PertAtm+PertOcn (2XCO2, Pert OHFC) includes the climatic effects of both CO_2 doubling and the ocean response to CO_2 doubling; this experiment produces a climate state similar to that in 2XCO2_300yr (see supporting information (SI) section S1). All perturbation SOM experiments are differenced from the Control SOM (1XCO2, Cont OHFC). Perturbation SOM experiments are compared to each other rather than the fully coupled 2XCO2_300yr experiment because SOM climatologies differ from fully coupled climatologies due to loss of high-frequency ocean variability (i.e., submonthly time scales) in the former. Each CESM-SOM experiment is run for 60 years, with seasonal climatologies constructed from the final 30 years.

3. Results

3.1. The Ocean Response to Quasi-Equilibrium CO_2 Doubling

With quasi-equilibrium CO_2 doubling, the OHFC and sea ice respond in a way that is strongly seasonal and remarkably similar between the Arctic and Antarctic. The winter OHFC shifts poleward in both hemispheres (Figures 1b and 1c), with OHFC decreasing equatorward of the climatological ice edge; the region of increased OHFC is coincident with regions of winter sea ice loss in both hemispheres, reflecting strong coupling between the OHFC and the ice edge (Bitz et al., 2005; Rose et al., 2013). In summer, on the other hand, the OHFC decreases modestly in both hemispheres with little relation to ice loss (Figures 1a and 1d).

Closer examination of the winter season response reveals regional and hemispheric differences in the OHFC and sea ice changes. In the Arctic, increased winter OHFC and ice loss are greatest in the Greenland, Barent, Bering, and Okhostk Seas; ice loss and increased OHFC extend nearly to the pole (Figure 1b). In the Antarctic, greater winter OHFC and ice loss are relatively evenly distributed around the continent; the smallest responses are in the Weddell and Ross Seas, where the OHFC increase is modest (Figure 1c).

The seasonal implied ocean heat transport (OHT) change at latitude ϕ_0 may be computed in the oceanic mixed layer using the mixed layer OHFC (Q_{flx}) as

$$\text{OHT}(\phi_0) = 2\pi r_{\text{Earth}}^2 \int_{-\pi/2}^{\phi_0} (Q_{\text{flx}}(\phi) - R_{\text{storage}}(\phi)) \cos\phi \, \text{d}\phi, \tag{2}$$

where r_{Earth} is the planetary radius and R_{storage} is the mixed layer heat storage. With CO_2 doubling, there is decreased winter OHT in the midlatitudes and subpolar regions but increased OHT closer to the poles in both hemispheres (Figure 1e). This response has been identified in the Arctic in a range of climate models (Holland & Bitz, 2003; Hwang et al., 2011) and has been attributed to decreased subpolar heat loss that results in more poleward ocean heat advection at higher latitudes (Nummelin et al., 2017). In the remainder of this study, we focus on the climate impact of this dynamic ocean response (i.e., changes in OHFC) that accompanies quasi-equilibrium CO_2 doubling. We leave further, more detailed, assessment of this ocean response for future work.

3.2. The Climate Impact of the Quasi-Equilibrium Ocean Response to CO_2 Doubling

When imposed in the CESM-SOM, the Pert OHFC (as computed from the fully coupled quasi-equilibrium CO_2 doubling experiment and imposed in PertOcn and PertAtm+PertOcn) produces a range of winter season climate impacts that modify the effects of CO_2 doubling by itself (i.e., without any ocean adjustments, as in PertAtm). These impacts are similar between the Arctic and Antarctic, and we outline them here.

First, imposing Pert OHFC warms the high latitudes and cools the lower latitudes in winter (colors, Figures 2a–2c and 2e–2g). Warming over the polar oceans and cooling over the subpolar areas are apparent in PertOcn (Figures 2b and 2f). Compared to PertAtm, PertAtm+PertOcn warms less in the midlatitudes and subpolar areas and warms more closer to the pole (compare Figures 2a and 2e to 2c and 2g; see also Figures 2d and 2h). In the Arctic, the high-latitude warming extends over the entire Arctic Ocean and surrounding boreal North America and Eurasia; Greenland, notably, cools. In the Antarctic, warming is focused around the periphery of the continent, with cooling over the Ross and Weddell Seas, and the continent itself. Extrapolar cooling is more extensive in the Northern Hemisphere (NH) than Southern Hemisphere (SH).

Greater polar amplification of warming is evident when Pert OHFC is imposed (Table 2, compare PertAtm+PertOcn and PertAtm), due to both greater warming over the polar regions and less warming over the extrapolar regions. The increase in polar amplification is more pronounced in the NH, where $\Delta T_{\text{polar}}/\Delta T_{\text{global}}$ over ocean increases from 3.0 to 3.6 (with ΔT_{polar} computed poleward of 65°N/65°S in the NH/SH) . The increase is smaller in the SH, where polar amplification over ocean increases from 1.5 to 1.6. While greater polar temperatures over ocean are evident in the SH in PertOcn, the climate response is less linear in the SH high latitudes than the NH (i.e., the sum of PertAtm and PertOcn differs notably from PertAtm+PertOcn; see SI section S2), and there is less Antarctic warming in PertAtm+PertOcn than in PertAtm (Table 2). This nonlinearity in the SH is due to a nonlinear cloud response, which damps the impact of Pert OHFC in the PertAtm+PertOcn experiment (see SI section S3).

In both hemispheres, the high-latitude warming due to Pert OHFC is also associated with decreased sea ice area (contours, Figures 2a–2c and 2e–2g). In general, ice loss is greater in both hemispheres when the

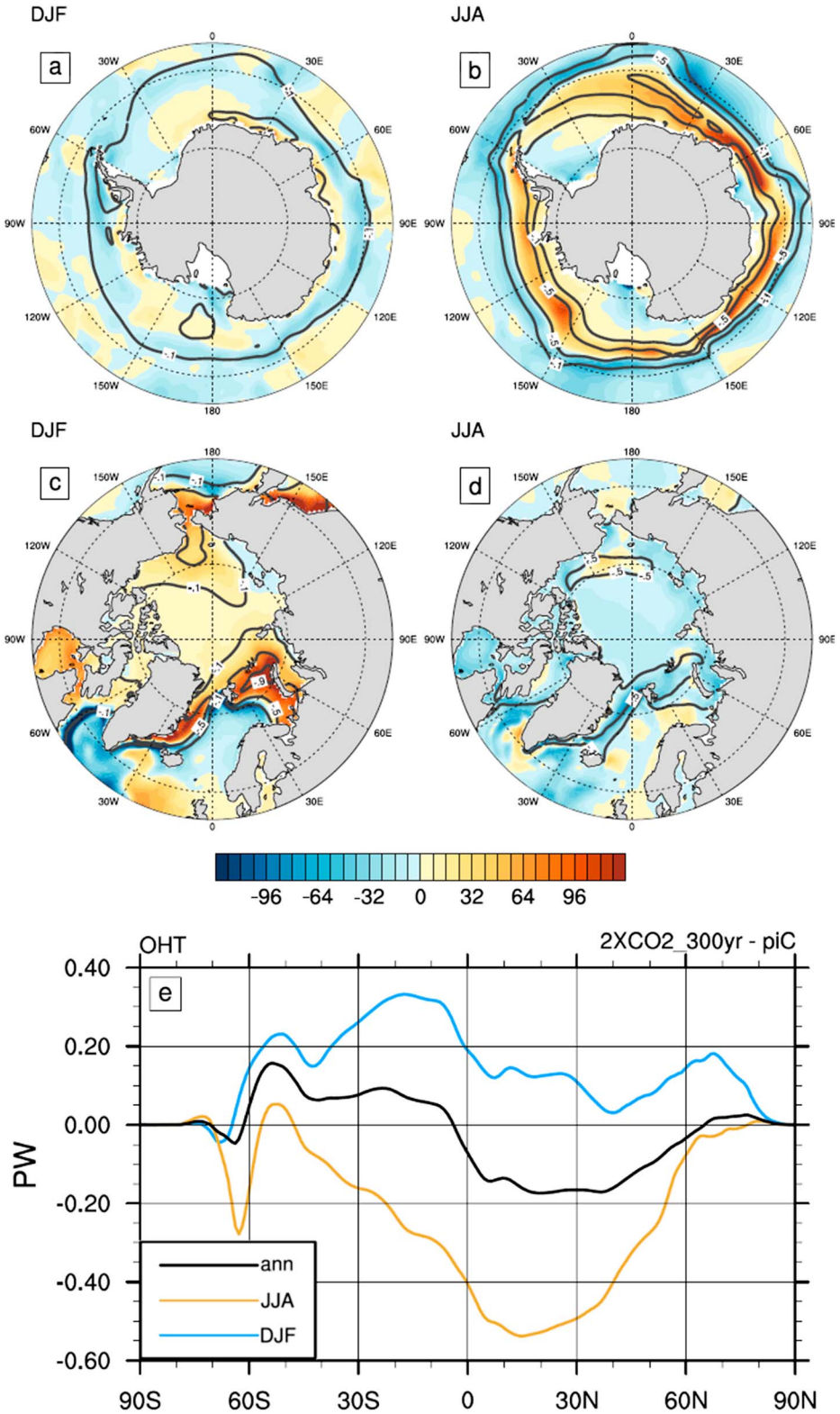

Figure 1. (a–d) Change in ocean heat flux convergence (OHFC) into the mixed layer (colors; in W m^{-2}) and change in sea ice concentration (contours at −0.1, −0.5, −0.9) between the preindustrial control (piC) simulation and the CO_2 doubling (2XCO2_300yr) simulation, for the Antarctic in (a) December, January, March (DJF) and (b) June, July, August (JJA) and Arctic in (c) DJF and (d) JJA. (e) Change in ocean heat transport in the mixed layer (2XCO2_300yr—piC; in PW) in DJF (yellow), JJA (blue), and the annual mean (black).

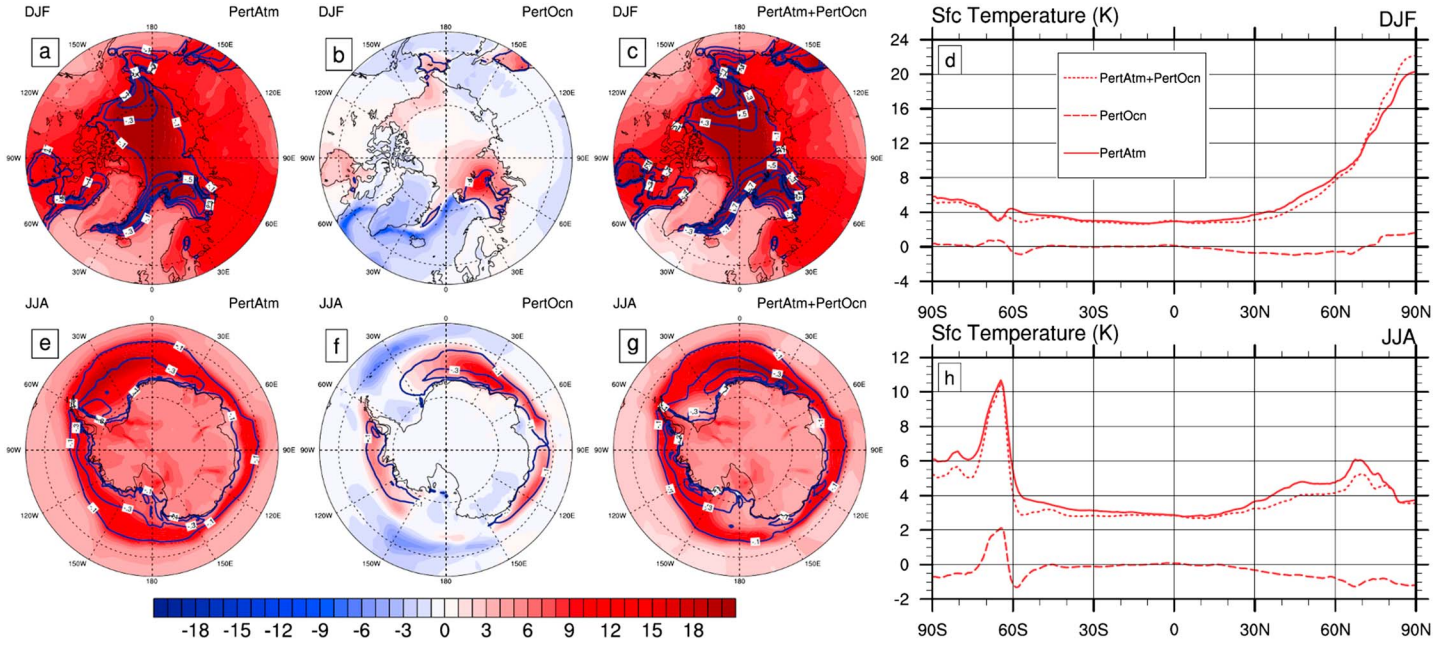

Figure 2. (a–c, e–g) Change in surface temperatures (colors; in K) and sea ice concentration (contours at −0.1, −0.3, −0.5, −0.7, −0.9) in DJF (Figures 2a–2c) and JJA (Figures 2e–2g) in the SOM perturbation experiments: PertAtm (Figures 2a and 2e), PertOcn (Figures 2b and 2f), and PertAtm+PertOcn (Figures 2c and 2g). (d, h) Zonal mean change in surface temperatures (in K) in DJF and JJA in the SOM perturbation experiments.

ocean response to CO_2 doubling is imposed (compare PertAtm to PertAtm+PertOcn, Figures 2a and 2e to 2c and 2g), with the spatial pattern of winter ice loss similar to that in the (fully coupled) 2XCO2_300yr experiment (compare Figures 2 to Figure 1). Overall, there is greater sea ice loss in the Arctic than in the Antarctic (a 17% reduction in Arctic sea ice area in PertAtm+PertOcn relative to PertAtm, compared to a 1% reduction in Antarctic sea ice area). Ice loss in the Antarctic is modest because there is an increase in sea ice concentration over the Ross and Weddell Seas that compensates for ice loss around the rest of the continent (Figures 2b and 2f).

At the surface, imposing Pert OHFC increases turbulent winter ocean-to-atmosphere heat fluxes closer to the pole in both hemispheres, thereby delivering more heat to the near-surface atmosphere at the high latitudes. Both sensible and latent heat fluxes are shifted poleward when the ocean response to CO_2 doubling is included (compare PertAtm+PertOcn to PertAtm, Figures 3a and 3b). As a result, the net ocean-to-atmosphere energy flux decreases equatorward of 70°N/65°S and increases poleward in the NH/SH. This poleward shift in the spatial pattern of the turbulent fluxes in winter mirrors the poleward shift in Pert OHFC relative to Cont OHFC (compare SI section S4 to Figures 1a and 1d) and is consistent with spatial covariance between latent heat fluxes and OHFC anomalies reported in previous studies (e.g., Sutton & Mathieu, 2002). Greater latent heat fluxes also increase the fraction of the polar precipitation due to locally sourced moisture, which drives a significant part of the polar hydrologic cycle change with CO_2 doubling (Singh et al., 2017).

Table 2
Temperature Change (Polar, ΔT_{polar}, and Global, ΔT_{global}) and Polar Amplification ($\Delta T_{polar}/\Delta T_{global}$) in the PertAtm and PertAtm+PertOcn SOM Perturbation Experiments (Relative to C)

Experiment name	Hemisphere (season)	ΔT_{polar}	ΔT_{global}	$\Delta T_{polar}/\Delta T_{global}$
PertAtm	NH (DJF)	12.8 K (7.5 K)	5.1 K (2.5 K)	2.5 (3.0)
PertAtm+PertOcn	NH (DJF)	13.4 K (8.2 K)	4.7 K (2.3 K)	2.8 (3.6)
PertAtm	SH (JJA)	7.9 K (4.4 K)	3.8 K (2.9 K)	2.1 (1.5)
PertAtm+PertOcn	SH (JJA)	7.2 K (4.2 K)	3.5 K (2.6 K)	2.1 (1.6)

Note. Polar regions are designated as poleward of 65°N or S. Temperature changes and polar amplification are given for ocean regions only in parentheses.

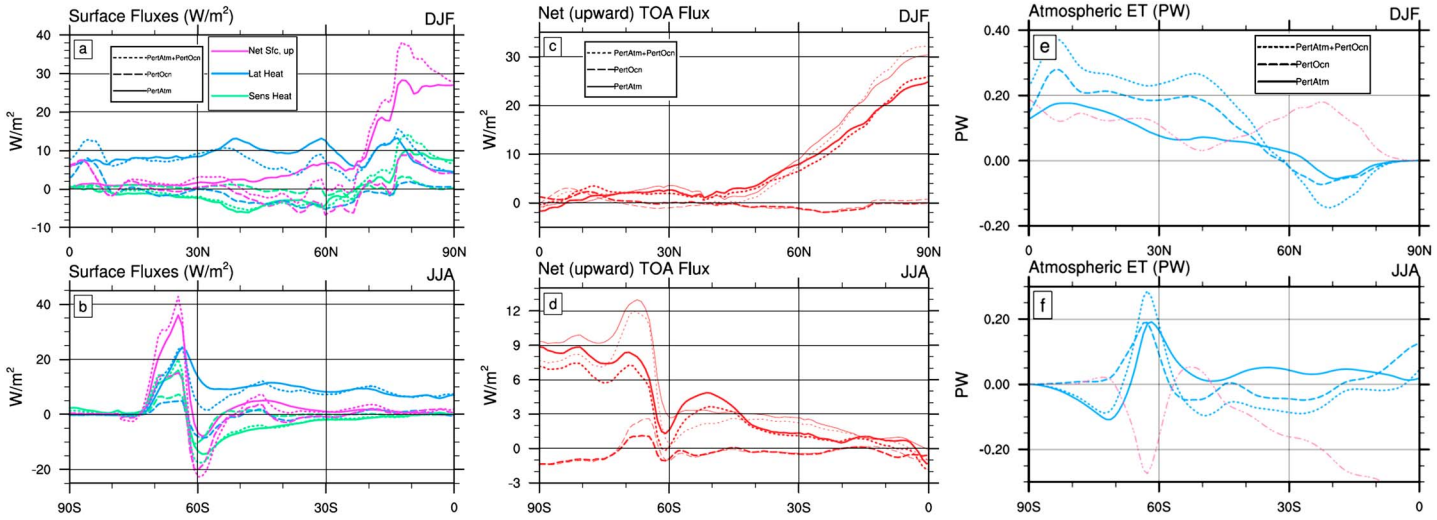

Figure 3. (a, b) Surface fluxes (in W m^{-2}), (c, d) top-of-atmosphere fluxes (in W m^{-2}), and (e, f) atmospheric energy transports (in PW; mixed layer OHT anomaly in 2XCO2_300yr shown in pink for comparison) for DJF (Figures 3a–3c) and JJA (Figures 3d–3f) in the SOM perturbation experiments (shown as the difference from the Control SOM). For TOA fluxes (Figures 3c and 3d), both all sky (thick lines) and clear sky (thin lines) are shown for each of the experiments.

At top-of-atmosphere (TOA), imposing Pert OHFC decreases energy loss to space at the high latitudes. Including the ocean response to CO_2 doubling decreases the net upward TOA flux in both polar and subpolar regions (compare PertAtm+PertOcn to PertAtm in Figures 3c and 3d). This decrease is mostly due, in polar winter, to a decrease in the all-sky outgoing longwave radiative flux (OLR), implying a decrease in atmospheric temperatures at the effective radiating level. The lone exception is poleward of 80°N in the Arctic, where OLR increases. In the NH, some of this reduction in the OLR can be attributed to greater cloudiness in PertAtm+PertOcn relative to PertAtm, as Pert OHFC is associated with greater clear-sky OLR poleward of 70°N (Figure 3c).

High-latitude meridional atmospheric energy transport (AET) changes compensate for the increased OHT implied by Pert OHFC. In all experiments, AET decreases over high-latitude oceans in winter, with a greater decrease in PertAtm+PertOcn relative to PertAtm (Figures 3e and 3f). In the Arctic, this amounts to a decrease in AET of 0.15 PW, while the decrease in the Antarctic is nearly 0.30 PW. These decreases in the AET are nearly equal and opposite to the increase in OHT implied by Pert OHFC (Figures 3e and 3f), indicating near-perfect compensation between high-latitude ocean and atmosphere energy transport anomalies in PertAtm+PertOcn (Bjerknes, 1964; Enderton & Marshall, 2009; Stone, 1978; Vellinga & Wu, 2008). Therefore, differences in the AET change between the Arctic and Antarctic reflect the differences in the OHT change implied by Pert OHFC. In the SH, the region of decreasing poleward AET is centered near 65°S, coincident with the region of increased OHT flanking the Antarctic continent; AET increases over the continent itself (Figure 3f). In the NH, on the other hand, the AET decline is centered near 70°N, and extends to the pole, mirroring the Arctic OHT change.

3.2.1. Feedback Analysis

To understand how Pert OHFC modifies high-latitude climates in winter, we perform a local radiative feedback analysis (as described in Armour et al., 2013), in which the feedback $\lambda_X(\phi)$ due to X at latitude ϕ is computed as

$$\lambda_X(\phi) = \left.\frac{\partial R_{\mathrm{TOA}}}{\partial X}\right|_{\phi,p} \frac{\Delta X(\phi,p)}{\Delta T_s(\phi)}, \tag{3}$$

where $\partial R_{\mathrm{TOA}}/\partial X|_{\phi,p}$ is the local radiative feedback kernel (computed from the CAM3; see Shell et al., 2008), $T_s(\phi)$ is the local surface temperature, and Δ denotes the difference between the experiment of interest and Control.

Longwave (LW) temperature and cloud feedbacks contribute to increased winter high-latitude warming evident in PertOcn (Figures 4a and 4b), while the LW water vapor feedback plays a very minor role. In both hemispheres, the lapse rate feedback is more positive over the polar regions in PertOcn relative to PertAtm,

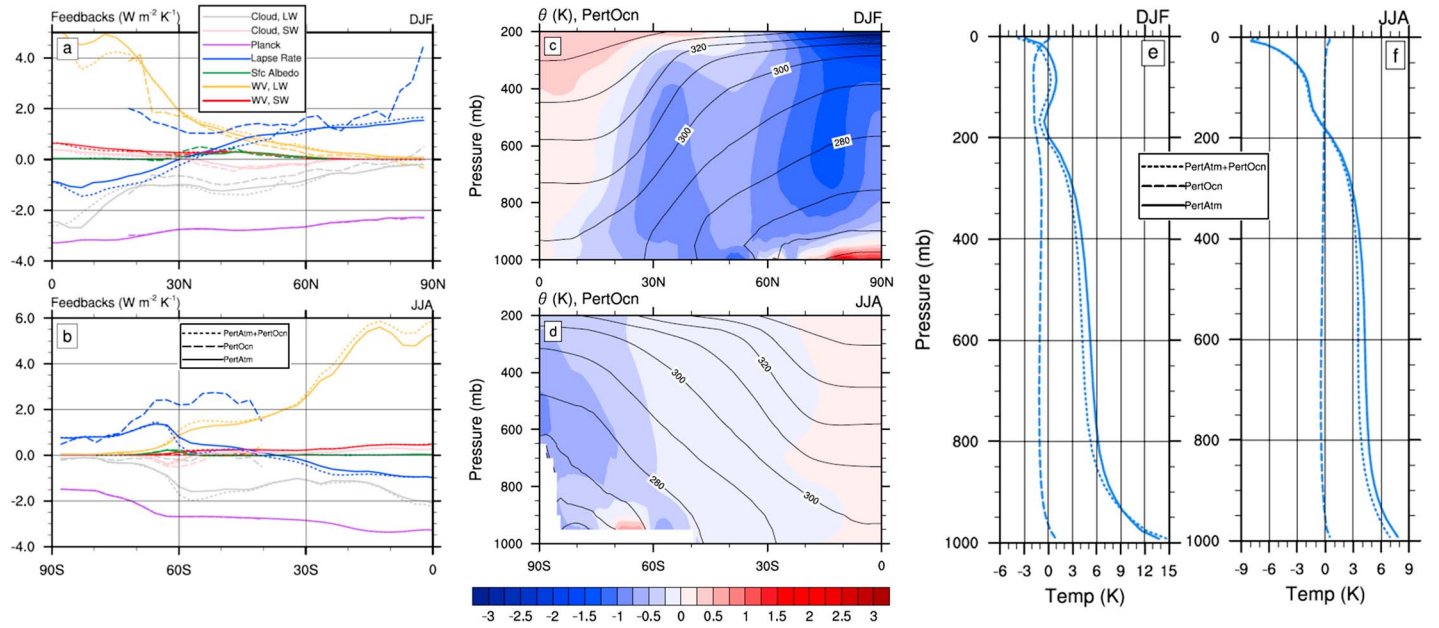

Figure 4. (a, b) Planck, lapse rate, surface albedo, longwave water vapor (WV, LW), shortwave water vapor (WV, SW), and cloud (SW and LW) radiative feedbacks (in W m^{-2} K^{-1}) in the SOM perturbation experiments (PertAtm in solid line, PertOcn in dashed line, and PertAtm+PertOcn in dotted line). Feedbacks are not computed where the surface temperature change, $\Delta T_s(\phi)$, is less than 0.2 K, which it is at many extrapolar latitudes in the PertOcn experiment. (c, d) Zonal mean potential temperature θ (in K) in the PertOcn experiment (lines) and its difference from the Control SOM (colors). (e, f) Polar (poleward of 65°N or 65°S) vertical temperature profile change (in K) between each of the SOM perturbation experiments and the control SOM. Shown for DJF (Figures 4a, 4c, and 4e) and JJA (Figures 4b, 4d, and 4f).

while LW cloud feedbacks are less negative (due to an increase in high clouds; see SI section S3). The high-latitude lapse rate feedback is greater over the polar oceans in PertAtm+PertOcn than in PertAtm in both hemispheres (by about 0.2 W m^{-2} K^{-1}, an increase of 13%), though the effect is more pronounced in the NH (resulting in ~5 W m^{-2} decrease in OLR poleward of 70° N). The (negative) longwave cloud feedback, on the other hand, is slightly less negative in PertAtm+PertOcn than PertAtm in the Arctic, but significantly more negative in the Antarctic, reflecting the role of the SH cloud response in moderating the impact of Pert OHFC there (see SI section S3).

The high-latitude lapse rate has been long identified as being crucial to polar-amplified warming (Manabe & Wetherald, 1975). In the polar regions, reduced warming aloft relative to the surface decreases the ability of the polar column to radiate energy to space locally and requires greater warming at the surface to compensate (Bintanja et al., 2011). In PertOcn, the polar midtroposphere cools in both hemispheres in response to Pert OHFC, which overlies the warmer surface (Figures 3c and 3d). Midlatitude and subpolar surface cooling in PertOcn, brought on by less ocean heat convergence in these regions, are mixed by eddies along isentropic surfaces to the polar midtroposphere (Laliberte & Kushner, 2013), decreasing AET (recall Figures 3e and 3f) and cooling the polar cap aloft. This cooling in the polar midtroposphere is also apparent in PertAtm+PertOcn relative to PertAtm (Figures 4e and 4f), reflecting cooler extrapolar regions in the former relative to the latter (recall Figures 2d and 2h). Thus, Pert OHFC amplifies the high-latitude lapse rate feedback in the Arctic and Antarctic by warming the surface while cooling the midtroposphere.

4. Discussion and Concluding Points

At quasi-equilibrium, CO_2 doubling shifts the winter season OHFC poleward in both hemispheres: less ocean heat converges in the midlatitudes and more ocean heat converges closer to the pole, coincident with the retreat of sea ice. Using a slab ocean configuration, we have shown that this OHFC change shifts turbulent ocean-to-atmosphere heat fluxes farther poleward, warms the high-latitude oceans, and erodes the sea ice edge. At the same time, the midlatitudes and subpolar areas cool, and this cooling is propagated to the polar midtroposphere; as a result, meridional atmospheric energy transport to the high latitudes decreases, energy loss to space at TOA decreases, and the (positive) lapse rate feedback is enhanced.

Our experiments directly show that ocean dynamics play a role in winter polar amplification with quasi-equilibrium CO_2 doubling, a finding consistent with previous model intercomparison studies (Holland & Bitz, 2003; Hwang et al., 2011). Changes in the OHFC instigate polar warming and extrapolar cooling, both of which play a part in the distinct response of polar climates to forcings (recall Table 2). The vertical structure of the winter polar atmosphere, characterized by a strong surface inversion and decoupling between the boundary layer and upper levels, tends to trap heat brought in by the ocean at the surface; simultaneously, less warming aloft, linked to extrapolar cooling, decreases the effectiveness of heat loss to space.

Our results imply that the ocean response to CO_2 doubling impacts high-latitude radiative feedbacks in winter, particularly those due to lapse rate and clouds. While radiative feedbacks may be assessed as a proximate cause of high-latitude climate sensitivity as in Pithan and Mauritsen (2014), these assessments do not reveal the ultimate cause of strong local feedbacks, which may be a result of large-scale dynamics. We have shown that an enhanced positive lapse rate feedback and, to a lesser extent, a diminished negative cloud feedback both characterize a dynamic ocean response to CO_2 doubling in which more heat is delivered into the high latitudes by the ocean.

Though we find that ocean dynamics play a role in polar-amplified warming in winter, we emphasize that the role is secondary to that of the atmosphere and the local oceanic mixed layer. Indeed, in the fully coupled CESM, absorbed shortwave radiation over the Arctic polar cap in summer increases by over 0.7 PW with CO_2 doubling; the OHT in winter, on the other hand, increases by less than 0.2 PW. For this reason, polar-amplified warming with CO_2 doubling and its attendant feedbacks are well approximated when the OHFC is held fixed (i.e., as in PertAtm).

We propose a mechanism by which ocean and atmospheric energy transport have opposing effects on high-latitude temperature amplification, as shown by Hwang et al. (2011). High-latitude ocean and atmosphere energy transport changes compensate in both hemispheres: increased ocean heat transport into the high latitudes is accompanied by decreased atmospheric energy transport. This partitioning of the energy transport change between atmosphere and ocean, in turn, impacts polar amplification: when more energy is transported poleward by the ocean and less by the atmosphere (as in PertAtm+PertOcn), there is greater polar amplification. This suggests a fundamental difference between ocean and atmospheric energy transports into the high latitudes, in that excess energy brought in by the ocean is more effective at raising surface temperatures than energy brought in by the atmosphere (see SI section S5; also see Cronin & Jansen, 2016).

Finally, we point out an important caveat of the interhemispheric parity we have noted in this study. Though the change in OHFC is similar between the Arctic and Antarctic, and the impact of this OHFC change is similar when imposed in the SOM framework in isolation, we have identified substantial nonlinearities in the response of the Antarctic to the anomalous OHFC when CO_2 is doubled. In particular, polar warming is muted in the Antarctic when CO_2 doubling and Pert OHFC are imposed simultaneously (i.e., PertAtm+PertOcn) because of a decrease in clouds over the Southern Ocean not instigated when Pert OHFC is imposed by itself (i.e., PertOcn; see SI section S3). In the Arctic, on the other hand, the climate response to Pert OHFC is similar between the preindustrial and doubled CO_2 atmospheric states, and no such mitigating cloud feedback exists. Many studies have highlighted model difficulties in simulating cloud cover over the Southern Ocean (see, e.g., Bodas-Salcedo et al., 2012) and during polar night (where accurate observations are difficult; see, e.g., Sassen et al., 2008; Winker et al., 2010), which suggests caution in generalizing these results. Further studies on the role of SH cloud feedbacks in high-latitude warming are required.

Several other caveats also remain. First, in the design of our study, we have treated Pert OHFC (i.e., the change in the OHFC associated with quasi-equilibrium CO_2 doubling) as a forcing. In reality, the ocean response to quasi-equilibrium CO_2 doubling depends on the atmosphere, ice, and land responses. Indeed, the covariance between regions of OHFC decrease and sea ice retreat (recall Figure 1) suggests strong coupling between these processes; studies that isolate a single system component are necessarily flawed. Second, we have only considered the quasi-equilibrium ocean response to CO_2 doubling, which has permitted us to consider interhemispheric parity in the high-latitude climate response; the transient response is where significant asymmetry between the hemispheres arises, given strong ocean heat uptake in the SH. Finally, we have presented results from the CESM, a single state-of-the-art climate model. Study of other models may modify the conclusions presented here. Despite these caveats, our work shows that changes in ocean dynamics impact the high-latitude climate system response to quasi-equilibrium CO_2 doubling, with significant parity between the hemispheres.

Acknowledgments
All authors thank Karen Shell for generously sharing her radiative feedback kernels with the research community. H.A.S. is grateful for funding from the Pacific Northwest National Laboratory's Linus Pauling Distinguished Postdoctoral Fellowship and thanks to Ruby Leung, Marika Holland, and Jian Lu for helpful advice and discussions. B.E.J.R. was supported by NSF grant AGS-1455071. All climate model data presented here have been made publicly available via the Zenodo data archive at http://doi.org/10.5281/zenodo.848261.

References

Armour, K., Bitz, C., & Roe, G. (2013). Time-varying climate sensitivity from regional feedbacks. *Journal of Climate*, *26*, 4518–4534.
Bailey, D., Hannay, C., Holland, M., & Neale, R. (2010). Slab ocean model forcing. (Tech. Rep.), Boulder, CO: National Center for Atmospheric Research.
Bintanja, R., Graverson, R., & Hazeleger, W. (2011). Arctic winter warming amplified by the thermal inversion and consequent low infrared cooling to space. *Nature Geoscience*, *4*, 758–760.
Bitz, C., Holland, M., Hunke, E., & Moritz, R. (2005). Maintenance of the sea ice edge. *Journal of Climate*, *18*, 2903–2921.
Bitz, C., Gent, P., Woodgate, R., Holland, M., & Lindsay, R. (2006). The influence of sea ice on ocean heat uptake in response to increasing CO_2. *Journal of Climate*, *19*, 2437–2450.
Bitz, C., Shell, K., Gent, P., Bailey, D., Danabasoglu, G., Armour, K., … Kiehl, J. (2012). Climate sensitivity in the community Climate System Model, version 4. *Journal of Climate*, *25*(9), 3053–70.
Bjerknes, J. (1964). Atlantic air-sea interaction. *Advances in Geophysics*, *10*, 1–82.
Bodas-Salcedo, A., Williams, K., Field, P., & Lock, A. (2012). The surface downwelling solar radiation surplus over the Southern Ocean in the Met Office model: The role of midlatitude cyclone clouds. *Journal of Climate*, *25*, 7467–7486.
Cronin, T., & Jansen, M. (2016). Analytic radiative-convective equilibrium as a model for high-latitude climate. *Geophysical Research Letters*, *43*, 449–457. https://doi.org/10.1002/2015GL067172
Danabasoglu, G., Bates, S., Briegleb, B., Jayne, S., Jochum, M., Large, W., … Yeager, S. (2012). The CCSM4 ocean component. *Journal of Climate*, *25*, 1361–1389.
Enderton, D., & Marshall, J. (2009). Explorations of atmosphere-ocean-ice climates on an aquaplanet and their meridional energy transports. *Journal of the Atmospheric Sciences*, *66*, 1593–1611.
Gent, P., & McWilliams, J. (1992). Isopycnal mixing in ocean circulation models. *Journal of Physical Oceanography*, *20*, 150–155.
Holland, M., & Bitz, C. (2003). Polar amplification of climate change in coupled models. *Climate Dynamics*, *21*, 221–232.
Hunke, E., & Lipscomb, W. (2008). CICE: The los alamos sea ice model, documentation and software, version 4.0 (Tech. Rep. LA-CC-06-012). Los Alamos, NM: Los Alamos National Laboratory.
Hurrell, J., Holland, M., Gent, P., Ghan, S., Kay, J., Kushner, P., … Marshall, S. (2013). The Community Earth System Model: A framework for collaborative research. *Bulletin of the American Meteorological Society*, *94*, 1339–1360.
Hwang, Y.-T., Frierson, D., & Kay, J. (2011). Coupling between Arctic feedbacks and changes in poleward energy transport. *Geophysical Research Letters*, *38*, L17704. https://doi.org/10.1029/2011GL048546.
Laliberte, F., & Kushner, P. (2013). Isentropic constraints by midlatitude surface warming on the Arctic midtroposphere. *Geophysical Research Letters*, *40*, 606–611. https://doi.org/10.1029/2012GL054306
Mahlstein, I., & Knutti, R. (2011). Ocean heat transport as a cause for model uncertainty in projected Arctic warming. *Journal of Climate*, *24*, 1451–1460.
Manabe, S., & Wetherald, R. (1975). The effects of doubling the CO_2 concentration on the climate of a general circulation model. *Journal of the Atmospheric Sciences*, *32*(1), 3–15.
Neale, R., Chen, C.-C., Gettelman, A., Lauritzen, P., Park, S., Williamson, D., & Taylor, M. A. (2012). Description of NCAR Community Atmosphere Model (CAM 5.0) (NCAR Tech. Note TN-486+STR), NCAR, Boulder, Colo.
Nummelin, A., Li, C., & Hezel, P. (2017). Connecting ocean heat transport changes from the midlatitudes to the Arctic Ocean. *Geophysical Research Letters*, *44*, 1899–1908. https://doi.org/10.1002/2016GL071333
Oleson, K., Lawrence, D., Bonan, G., Flanner, M., Kluzek, E., Lawrence, P., … Zeng, X. (2010). Technical description of version 4.0 of the Community Land Model (CLM) (Tech. Rep. TN-478+STR), National Center for Atmospheric Research, Boulder, Colo.
Pithan, F., & Mauritsen, T. (2014). Arctic amplification dominated by temperature feedbacks in contemporary climate models. *Nature Geoscience*, *7*, 181–184.
Purkey, S., & Johnson, G. (2010). Warming of global abyssal and deep southern ocean waters between the 1990s and 2000s: Contributions to global heat and sea level rise budgets. *Journal of Climate*, *23*, 6336–6351.
Rose, B., Ferreira, D., & Marshall, J. (2013). The role of oceans and sea ice in abrupt transitions between multiple climate states. *Journal of Climate*, *26*, 2862–2879.
Rose, B., Armour, K., Battisti, D., Feldl, N., & Koll, D. (2014). The dependence of transient climate sensitivity and radiative feedbacks on the spatial pattern of ocean heat uptake. *Geophysical Research Letters*, *41*, 1071–1078. https://doi.org/10.1002/2013GL058955
Sassen, K., Wang, Z., & Liu, D. (2008). Global distribution of cirrus clouds from Cloudsat/Cloud-Aerosol Lidar and Infrared Pathfinder Satellite Observations (CALIPSO) measurements. *Journal of Geophysical Research*, *113*, D00A12. https://doi.org/10.1029/2008JD009972
Shell, K., Kiehl, J., & Shields, C. (2008). Radiative kernel technique to calculate climate feedbacks in NCAR's Community Atmospheric Model. *Journal of Climate*, *21*, 2269–2283.
Singh, H., Bitz, C., Donohoe, A., & Rasch, P. (2017). A source-receptor perspective on the polar hydrologic cycle: Source regions, seasonality, and Arctic-Antarctic parity in the hydrologic cycle response to co_2-doubling. *Journal of Climate*. https://doi.org/10.1175/JCLI-D-16-0917.1
Stone, P. (1978). Constraints on dynamical transports of energy on a spherical planet. *Dynamics of Atmospheres and Oceans*, *2*, 123–139.
Sutton, R., & Mathieu, P.-P. (2002). Response of the atmosphere-ocean mixed-layer system to anomalous ocean heat-flux convergence. *Quarterly Journal of the Royal Meteorological Society*, *128*, 1259–1275.
Vellinga, M., & Wu, P. (2008). Relations between northward ocean and atmosphere energy transports in a coupled climate model. *Journal of Climate*, *21*, 561–575.
Winker, D., Pelon, J., Coakley, J., Ackerman, S., Charlson, R., Colarco, P., … Wielicki, B. (2010). The CALIPSO mission: A 3D view of aerosols and clouds. *Bulletin of the American Meteorological Society*, *91*, 1211–1229.
Winton, M. (2006). Amplified Arctic climate change: What does surface albedo feedback have to do with it? *Geophysical Research Letters*, *33*, L03701. https://doi.org/10.1029/2005GL025244.